

<i>NDA</i>	19785	<i>Submission Date(s)</i>	October 29, 2007
<i>Brand Name</i>	Cardiolite; Technetium Tc99m-Sestamibi		
<i>Generic Name</i>	N/A		
<i>Reviewer</i>	Christy S. John, Ph.D		
<i>Team Leader</i>	Young Moon Choi, Ph.D.		
<i>OCP Division</i>	V		
<i>ORM Division</i>	Division of Medical Imaging and Hematology Drug Products		
<i>Sponsor</i>	Bristol-Myers Squibb Medical Imaging (BMS MI)		
<i>Relevant IND(s)</i>	28,333		
<i>Submission Type; Code</i>	SE5-018		
<i>Dose and Route of administration</i>	One day study 0.1-0.2 mCi/kg for rest, 0.3 mCi/kg for stress. Two days study 0.2 mCi/kg for rest and 0.2 mCi/kg for stress on day two; Intravenous injection		
<i>Indication</i>	Cardiolite is a myocardial perfusion imaging agent for rest and stress imaging of myocardium in patients with coronary artery disease		

Table of Contents

1	Executive Summary	3
1.1	Recommendations	3
1.2	Phase IV Commitments	3
1.3	Summary of Clinical Pharmacology Findings	4
2	Question-Based Review	5
2.1	General Attributes of the drug	5
2.2	General Clinical Pharmacology	7
2.3	Intrinsic Factors	15
2.4	Extrinsic Factors	16
2.5	General Biopharmaceutics	16
3	Detailed Labeling Recommendations	16
4	Appendices	17
4.1	Proposed Package Insert (Original and Annotated)	18
4.2	Individual Study Reviews	41
4.3	Consult Reviews (including Pharmacometric Reviews)	50

1 Executive Summary

Cardiolite was approved by FDA in 1990 for the rest and stress myocardial perfusion imaging in patients with coronary artery disease. In August 2001, BMS MI submitted a Proposed Pediatric Study Request (PPSR) for the study of Cardiolite® in pediatric patients. [REDACTED]

FDA issued a Written Request (WR) based on the recommendation of the Pediatric Advisory Subcommittee in December 2004 that required three pediatric studies in patients with Kawasaki Disease (KD).

The objectives of the WR were, 1) To determine the dosimetry, pharmacokinetics (PK), and safety of Tc^{99m} Sestamibi in pediatric patients, 2) To determine the diagnostic efficacy & safety of Tc^{99m} Sestamibi in pediatric patients with Kawasaki disease, by using clinical outcomes as the gold standard, 3) To determine the diagnostic efficacy and safety of Tc^{99m} Sestamibi in pediatric patients with Kawasaki disease, by using X-ray angiography as the gold standard.

The clinical pharmacology review focused on Study 1 and the results of dosimetry, PKs and biodistribution and found the following;

- 1) The radioactivity following Cardiolite® administration had similar blood PK profiles in children and adolescents. The blood PK profiles were significantly different between rest & stress subjects in both children and adolescent (p=0.0013).
- 2) In general, the radiation absorbed doses for various organs for children and adolescents were two to three fold higher than adults. These differences are due to body weight differences. Therefore, a body weight adjusted dose is given to pediatric subjects to obtain similar radiation absorbed dose in adults and pediatrics.

1.1.1 Recommendations:

The Office of Clinical Pharmacology/Division of Clinical Pharmacology 5 has reviewed the pediatric study submitted in NDA 19-785 (Supplement 018). The sponsor has performed the PK, biodistribution and dosimetry study as recommended in the Written Request. The application is acceptable from clinical pharmacology perspective provided the labeling recommendations are incorporated in the label. (See Detailed Labeling Recommendation).

1.2 Phase IV Commitments: N/A

Signature

Reviewer: Christy S. John, Ph.D.

Team Leader: Young Moon Choi, Ph.D.

Division Director: NAM Atiqur Rahman, Ph.D.

1.3 Summary of Clinical Pharmacology Findings:

The clinical pharmacology team reviewed Study 1. The goals of this study were to determine the dosimetry, pharmacokinetics (biodistribution in blood and urine) and safety of Technetium Tc99m Sestamibi in pediatric patients.

The radioactivity following Cardiolite® administration demonstrated similar blood PK profiles in children and adolescents, whereas the profiles were significantly different between rest and stress subjects ($p=0.0013$). The overall blood PK profiles were the same as for children, adolescent and adults.

The mean %ID (Injected Dose) in whole body blood volume (WBBV) was 53.5% at 1 minute in stress subjects followed by a rapid decline to 5.1% at 5 minutes, compared to that of 28.4% at 1 minute and 5.4% at 5 minutes in rest subjects. The exposure to radioactivity in blood following Cardiolite administration was 6.59 ± 2.59 %ID.hr, the terminal elimination half-life ($T_{1/2}$) was 3.45 ± 1.13 hours, and the mean residence time (MRT) of 3.62 ± 1.27 hours. Higher AUC values were observed in stress subjects and in children with differences that were statistically significant. No significant differences were observed in terminal elimination $T_{1/2}$ and MRT values. The overall mean urinary excretion of radioactivity by 6 hours was $13.8 \pm 8.59\%$, with the majority recovered during the first two hours post-Cardiolite® administration. The radiation dosimetry estimates for individual organs were calculated from analysis of whole-body image data taken at four time points after injection. Anterior and posterior whole-body Cardiolite conjugate images were obtained with a dual-head gamma camera using Cardiolite at 15 min, 1.5 hr, 4 hr and 8 hours. Image data were quantified based upon the Medical Internal Radiation Dose (MIRD) methodology. Organ thickness values required for determining attenuation correction factors were taken from Cristy-Eckerman pediatric phantoms. Absorbed dose estimates were produced from the standard MIRD methodology using Organ Level Internal Dose Assessment/Exponential Modeling (OLIDA/EXM).

In general, the radiation absorbed doses for various organs for children and adolescents were two to three fold higher than adults. These differences are due to body weight differences. Therefore, a body weight adjusted dose is given to pediatric subjects, so that a similar radiation absorbed dose is found in adults and pediatrics. The organs receiving the highest doses were those that formed the hepatobiliary excretion pathways; those are upper large intestine wall receiving 10-12 rads/30 mCi dose; small intestine receiving 6-7 rads/30 mCi dose; and gall bladder receiving 5-6 rads/30 mCi dose.

2 Question Based Review

2.1 General Attributes of Drug

What are the general attributes of the drug Cardiolite® (Technetium-Tc^{99m}-Sestamibi for injection)?

Cardiolite® (Kit for the Preparation of Technetium Tc^{99m} Sestamibi for Injection) is a freeze dried kit, to be reconstituted with sterile, non-pyrogenic, oxidant-free Sodium Pertechnetate Tc^{99m}, (NaTcO₄). The pH of the reconstituted product is 5.5 (5.0-6.0). No bacteriostatic preservative is present in the kit. The precise structure of the technetium complex is Tc^{99m} [MIBI]₆⁺, where MIBI is 2-methoxy isobutyl isonitrile. Technetium Tc^{99m} decays by isomeric transition with a physical t_{1/2} of 6.02 hours.

2.1.1 What pertinent regulatory background or history contribute to the current assessment of the clinical pharmacology of Cardiolite?

Cardiolite was approved by the FDA in 1990 for the rest and stress myocardial perfusion imaging in patients with coronary artery disease. In August 2001, BMS MI submitted a Proposed Pediatric Study Request (PPSR) for the study of Cardiolite® in pediatric patients. [REDACTED]

[REDACTED] Subsequently, FDA indicated their wish to seek external advice, and convened a meeting of the Pediatric Advisory Subcommittee (PAS) of the Anti-Infective Drugs Advisory Committee in February 2004. The subcommittee recommended that the pediatric patients with Kawasaki disease would benefit from studies utilizing Tc^{99m} myocardial perfusion imaging (MPI) agents such as Cardiolite®.

Following the PAS meeting, the FDA and BMS MI held several meetings to discuss appropriate dosing, efficacy, and safety study designs, including assessing diagnostic

accuracy and prognostic outcomes, that would benefit a pediatric population with Kawasaki Disease (KD). These discussions led to a further PPSR submission specifically focused on children with KD, and the FDA issued a WR in December 2004 that defined three pediatric studies in patients with KD. The 3 study protocols were submitted to the FDA. After the initiation of the pediatric studies, BMS MI submitted several amendments to the WR to best reflect clinical practice and facilitate study success. BMS MI submitted proposed amendments along with supporting documentation to the FDA. The FDA issued WR Amendment 02 in July 2007.

2.1.2 What are the highlights of the chemistry and physicochemical properties of the drug substance, and the formulation of the drug product as they relate to the clinical pharmacology of the drug?

Tc^{99m} Sestamibi is a cationic Tc^{99m} complex found to accumulate in viable myocardial tissue in a manner analogous to that of thallous chloride Tl²⁰¹. Scintigraphic images obtained in humans after the IV administration of the drug are comparable to those obtained with thallous chloride (Tl-201) in normal and abnormal myocardial tissue. Tc^{99m}-sestamibi crosses the cell membrane passively & accumulates in myocytes. It is eventually taken up by the mitochondria. The uptake of Tc^{99m}-sestamibi is related directly to the blood flow to the myocardium.

2.1.2 What are the proposed dosage(s) and route of administration?

Depending upon the clinical practice of an institution, imaging can be performed by One day protocol or Two day protocol.

One day study used 0.1-0.2 mCi/kg for rest, 0.3 mCi/kg for stress via intravenous administration.

Two day study used 0.2 mCi/kg for rest and 0.2 (isn't this 0.3) mCi/kg for stress on day two via intravenous injection.

2.1.3 What are the proposed mechanism(s) of action and therapeutic indication?

Tc^{99m} sestamibi passively crosses cell membranes. Animal studies have shown that myocardial uptake is not blocked when the sodium pump mechanism is inhibited. Although studies of subcellular fractionation and electron micrographic analysis of heart cell aggregates suggest that Tc^{99m} Sestamibi cellular retention occurs specifically within the mitochondria as a result of electrostatic interactions, the clinical relevance of these findings has not been determined.

2.2

General Clinical Pharmacology:

2.2.1 What are the design features of clinical pharmacology?

This was a Proposed Pediatric Study Request (PPSR) for the study of Cardiolite® in pediatric patients. In the PK study the sponsor was asked to perform a basic PK and dosimetry in pediatric subjects.

The PK study was an open label, non-randomized multi-center trial in pediatric patients who have been scheduled to undergo rest or exercise induced stress Tc^{99m} Sestamibi cardiac imaging. All patients underwent either whole body nuclear imaging to determine dosimetry; or assessment of PKs (biodistribution in blood and urine); or both. All patients were assessed for safety.

Age Groups studied:

Study 1: 2 independent groups of pediatric patients:

- 4 years to < 12 years
- 12 years to < 17 years

The sponsor was asked to study a minimum of 24 patients for safety and for either dosimetry, or PKs. This should include at least 12 patients in each group (children aged 4-11 years; adolescents aged 12 to < 17 years). Of these, at least 6 patients in each age group should be studied at rest and at least 6 studied during stress (4 cohorts: child rest, child stress, adolescent rest, adolescent stress). 6 patients in each of these cohorts should be evaluable for dosimetry or PK. At least 10 patients should be evaluated for both, dosimetry & PKs. All patients should be assessed for safety.

2.2.2 What is the basis for selecting the response endpoints, i.e, clinical or surrogate endpoints, or biomarkers (collectively called PD) and how are they measured in clinical pharmacology and clinical studies?

There was no efficacy or surrogate end-point collected in the Study 1. However, in Study 2 the diagnostic efficacy and safety of Tc^{99m} Sestamibi in pediatric patients with Kawasaki disease, using clinical outcomes as the truth standard was determined. Furthermore, in Study 3 the diagnostic efficacy and safety of Tc^{99m} Sestamibi in pediatric patients with Kawasaki disease was determined, using X-ray angiography as the gold standard.

2.2.4 Exposure-response Evaluation

2.2.4.1 What are the characteristics of the exposure-response relationships (dose-response, concentration-response) for efficacy? If relevant, indicate the time to the onset and offset of the desirable pharmacological response or clinical endpoint.

N/A. No exposure-response evaluated. PK and dosimetry alone were evaluated.

2.2.4.2 What are characteristics of the exposure-response relationship (dose-response, concentration-response) for safety?

N/A

2.2.4.3 Does this drug prolong QT or QTc interval?

N/A

2.2.4.4 Is the dose and dosing regimen selected by the sponsor consistent with the known relationship between dose-concentration-response, and are there any unresolved dosing or administration issues?

The dose selected by the sponsor for pediatric study was based upon the dose reported used in pediatric studies in the literature. There are no unresolved issues with the dosing or administration.

2.2.5 Pharmacokinetic Characteristics

2.2.5.1 What are the PK characteristics of the drug and its major metabolite?

For the 46 subjects in this study, the radioactivity following Cardiolite® administration had similar blood PK profiles in children and adolescents. In both groups, the profiles were significantly different between rest and stress subjects ($p=0.0013$). The mean %ID in whole body blood volume (WBBV) was 53.5% at 1 minute in stress subjects followed by a rapid decline to 5.1% at 5 minutes, compared to that of 28.4% at 1 minute and 5.4% at 5 minutes in rest subjects. A similar trend was observed in 18 subjects in the dosimetry and pharmacokinetic. The mean \pm standard deviations (SD) of the blood PK parameters for the PE population are summarized in the Table I for the 4 analysis groups.

Table I. PK parameters for Cardiolite in pediatric subjects

Analysis Groups	AUC(0-T) (%ID hr) Mean (SD)	AUC(INF) (%ID hr) Mean (SD)	Terminal T1/2 (hr) Mean (SD)	MRT (hr) Mean (SD)
Rest Children (n = 13)	5.21 (1.81)	6.86 (2.85)	3.50 (1.20)	3.73 (1.35)
Rest Adolescents (n = 14)	4.04 (1.37)	5.13 (1.65)	3.13 (0.84)	3.51 (1.12)
Stress Children (n = 10)	6.11 (1.97)	8.20 (3.07)	4.13 (1.19)	4.22 (1.32)
Stress Adolescents (n = 9)	5.43 (1.32)	6.66 (1.82)	3.10 (1.17)	2.96 (1.19)
Overall (n = 46)	5.09 (1.76)	6.59 (2.59)	3.45 (1.13)	3.62 (1.27)

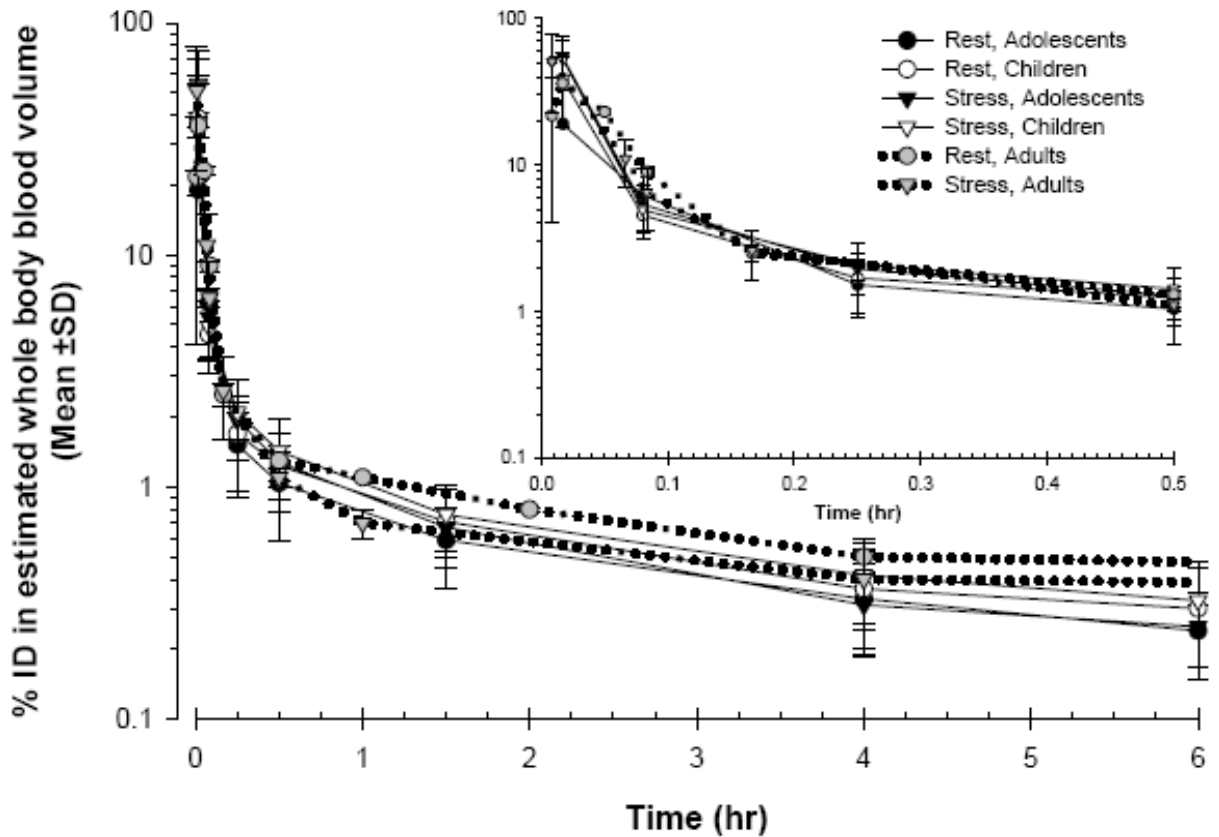


Figure 1. Pharmacokinetics of Tc-99m-sestamibi in blood in adults, adolescents, and children at rest and stress after IV administration.

The pharmacokinetic profiles of Tc-99m-sestamibi in blood in adults, adolescents, and children at rest and stress after IV administration exhibited very similar clearance profile. The data used for adults was derived from the published literature for 17 adults (Figure 1).

Rest/stress effect was significant in the models of residence time in the liver ($p=0.0025$), Small Intestine (SI) contents ($p=0.0015$), and Upper large intestine (ULI) ($p=0.002$). This was consistent with the visual observations of shifts of radioactivity between rest and stress studies in the organs of the hepatobiliary pathway. The overall mean urinary excretion of radioactivity by 6 hours was $13.8 \pm 8.59\%$, with the majority recovered during the first 2 hours post-Cardiolite® administration.

For %ID corrected for radioactive decay, myocardial %ID reached a value of approximately 1.5% to 2% at 15 minutes after injection, decreasing to about 1.2% at 4 hours. In lungs, the %ID was low, with a maximum of approximately 4.6% at 15 minutes after injection. Similar %ID values in the myocardium and lung were obtained between all analysis groups. Liver %ID was similar in both children and adolescents, but significant differences ($p<0.0001$) were observed between rest and stress. In rest subjects, the %ID in the liver decreased rapidly from a maximum of approximately 26% at 15 minutes to less than 9% at 90 minutes. With stress, values decreased from 15% at 15 minutes to 7% at 90 minutes. Significant differences between rest and stress of a similar magnitude were also observed ($p=0.0002$) in the SI contents.

2.2.5.2 How do the radiation absorbed doses for various organs for children and adolescent compare to the radiation absorbed dose for the adults?

For 47 Dosimetry Evaluable (DE) subjects, the largest mean estimated organ absorbed dose in this study was to the upper large intestine (ULI) wall at 0.082 mSv/MBq (0.30 rem/mCi). The next largest absorbed organ doses in decreasing order were to the small intestine (SI) wall at 0.043 mSv/MBq (0.16 rem/mCi), to the gall bladder wall at 0.042 mSv/MBq (0.16 rem/mCi), and to the lower large intestine wall at 0.035 mSv/MBq (0.13 rem/mCi). Significant differences were observed in liver, ULI contents, and SI contents between rest and stress subjects (liver: $p=0.026$; ULI: $p=0.015$; SI: $p=0.0002$) and between children and adolescents (liver: $p<0.0001$; ULI: $p=0.0016$; SI: $p<0.0001$). The average effective-dose equivalent (EDE) for Cardiolite®, which was a measure of stochastic risk, was estimated to be 0.019 mSv/MBq (0.072 rem/mCi). The average effective dose (ED) for Cardiolite®, which was also a measure of stochastic risk, was estimated to be 0.015 mSv/MBq (0.055 rem/mCi). Mean ED was significantly higher in children than in adolescents ($p<0.0001$). Similarly, mean EDE was significantly

higher in children than in adolescents ($p < 0.0001$). The radiation absorbed dose for children and adolescents at rest and stress are given in Table II and Table III, respectively.

Table II. Estimated Radiation Absorbed Dose in Adolescents and Children from CARDIOLITE[®] Rest Imaging

Organ	REST			
	Child (4 - 12 years)		Adolescent (13-16 years)	
	Rad / 30 mCi	mGy / 1110 MBq	Rad / 30 mCi	mGy / 1110 MBq
Adrenals	1.0	9.7	0.7	7.1
Brain	0.2	2.5	0.2	1.8
Breasts	0.3	3.1	0.2	2.2
Gallbladder Wall	6.8	68.2	4.3	43.4
Lower Large Intestine Wall	6.0	59.5	3.0	30.4
Small Intestine	7.6	76.2	4.2	42.4
Stomach Wall	1.2	12.1	0.8	8.2
Upper Large Intestine Wall	12.8	127.7	8.8	87.6
Heart Wall	1.2	11.7	1.0	9.7
Kidneys	3.0	30.1	2.4	24.3
Liver	2.1	20.7	1.5	14.8
Lungs	1.0	10.1	0.8	8.0
Muscle	0.6	6.3	0.4	4.4
Ovaries	2.7	27.4	1.8	17.7
Pancreas	1.3	12.6	0.9	8.5
Red Marrow	1.2	11.5	0.9	8.8
Bone Surfaces	1.4	14.0	1.1	10.7
Salivary Glands	1.0	9.9	0.5	5.1
Skin	0.3	3.0	0.2	2.0
Spleen	1.6	15.5	1.3	12.8
Testes	0.5	5.4	0.3	3.1
Thymus	0.4	3.7	0.3	2.9
Thyroid	0.8	8.0	0.6	5.9
Urinary Bladder Wall	4.2	41.7	2.2	22.3
Uterus	2.3	23.4	1.4	14.1
Total Body	0.8	8.3	0.6	5.7
Effective Dose	2.3	22.7	1.4	14.0
Effective Dose Equivalent	3.0	30.0	1.9	19.3

Table III. Estimated Radiation Absorbed Dose in Adolescents and Children from CARDIOLITE[®] During Stress Imaging

Organ	STRESS			
	Child (4 - 12 years)		Adolescent (13-16 years)	
	Rad / 30 mCi	mGy / 1110 MBq	Rad / 30 mCi	mGy/ 1110 MBq
Adrenals	1.1	10.7	0.7	6.5
Brain	0.4	4.4	0.3	2.6
Breasts	0.5	4.5	0.3	2.8
Gallbladder Wall	4.9	49.0	2.9	28.9
Lower Large Intestine Wall	4.0	40.3	2.6	25.7
Small Intestine	5.0	50.1	2.7	26.5
Stomach Wall	1.2	12.2	0.7	7.2
Upper Large Intestine Wall	10.2	102.4	5.2	51.9
Heart Wall	1.6	15.5	1.1	11.1
Kidneys	3.1	31.2	1.8	18.1
Liver	1.9	19.3	1.1	10.9
Lungs	1.3	12.7	0.8	8.4
Muscle	0.7	7.1	0.4	4.4
Ovaries	2.2	21.6	1.3	13.3
Pancreas	1.3	12.8	0.8	7.6
Red Marrow	0.7	7.3	0.6	5.6
Bone Surfaces	1.5	15.4	1.1	10.8
Salivary Glands	0.8	8.0	0.3	3.2
Skin	0.4	4.0	0.2	2.4
Spleen	1.5	15.2	1.0	9.9
Testes	0.7	6.6	0.4	3.8
Thymus	0.6	5.8	0.4	3.9
Thyroid	1.3	12.7	0.7	6.6
Urinary Bladder Wall	3.8	38.0	2.2	22.3
Uterus	2.0	19.5	1.1	11.3
Total Body	0.9	8.7	0.5	5.3
Effective Dose	1.9	19.3	1.1	11.1
Effective Dose Equivalent	2.5	24.8	1.4	13.6

Radiation dosimetry calculations performed using OLINDA/EXM by [REDACTED]

Table IV. Radiation absorbed doses from Tc-99m- sestamibi for adults (from current package insert)

Organ	Estimated Radiation Absorbed Dose			
	REST			
	2.0 hour void		4.8 hour void	
	rads/ 30 mCi	mGy/ 1110 MBq	rads/ 30 mCi	mGy/ 1110 MBq
Breasts	0.2	2.0	0.2	1.9
Gallbladder Wall	2.0	20.0	2.0	20.0
Small Intestine	3.0	30.0	3.0	30.0
Upper Large Intestine Wall	5.4	55.5	5.4	55.5
Lower Large Intestine Wall	3.9	40.0	4.2	41.1
Stomach Wall	0.6	6.1	0.6	5.8
Heart Wall	0.5	5.1	0.5	4.9
Kidneys	2.0	20.0	2.0	20.0
Liver	0.6	5.8	0.6	5.7
Lungs	0.3	2.8	0.3	2.7
Bone Surfaces	0.7	6.8	0.7	6.4
Thyroid	0.7	7.0	0.7	2.4
Ovaries	1.5	15.5	1.6	15.5
Testes	0.3	3.4	0.4	3.9
Red Marrow	0.5	5.1	0.5	5.0
Urinary Bladder Wall	2.0	20.0	4.2	41.1
Total Body	0.5	4.8	0.5	4.8

STRESS

Organ	2.0 hour void		4.8 hour void	
	rads/ 30 mCi	mGy/ 1110 MBq	rads/ 30 mCi	mGy/ 1110 MBq
Breasts	0.2	2.0	0.2	1.8
Gallbladder Wall	2.8	28.9	2.8	27.8
Small Intestine	2.4	24.4	2.4	24.4
Upper Large Intestine Wall	4.5	44.4	4.5	44.4
Lower Large Intestine Wall	3.3	32.2	3.3	32.2
Stomach Wall	0.6	5.3	0.5	5.2
Heart Wall	0.5	5.6	0.5	5.3
Kidneys	1.7	16.7	1.7	16.7
Liver	0.4	4.2	0.4	4.1
Lungs	0.3	2.6	0.2	2.4
Bone Surfaces	0.6	6.2	0.6	6.0
Thyroid	0.3	2.7	0.2	2.4
Ovaries	1.2	12.2	1.3	13.3
Testes	0.3	3.1	0.3	3.4
Red Marrow	0.5	4.6	0.5	4.4
Urinary Bladder Wall	1.5	15.5	3.0	30.0
Total Body	0.4	4.2	0.4	4.2

Radiation dosimetry calculations performed by Radiation Internal Dose Information Center, Oak Ridge Institute for Science and Education, PO Box 117, Oak Ridge, TN 37831-0117, (865) 576-3448.

2.2.5.3 What are the characteristics of drug metabolism?

Cardiolite does not undergo any metabolism.

2.3 Intrinsic Factors

2.3.1 What intrinsic factors (such as renal and hepatic dysfunction) influence pharmacokinetics (exposure)?

N/A. The sponsor has not studied influence of any intrinsic factors on pharmacokinetics.

2.4 Extrinsic Factors

2.4.1. What extrinsic factors such as gender, weight, smoking etc influence pharmacokinetics of Tc-99m-sestamibi?

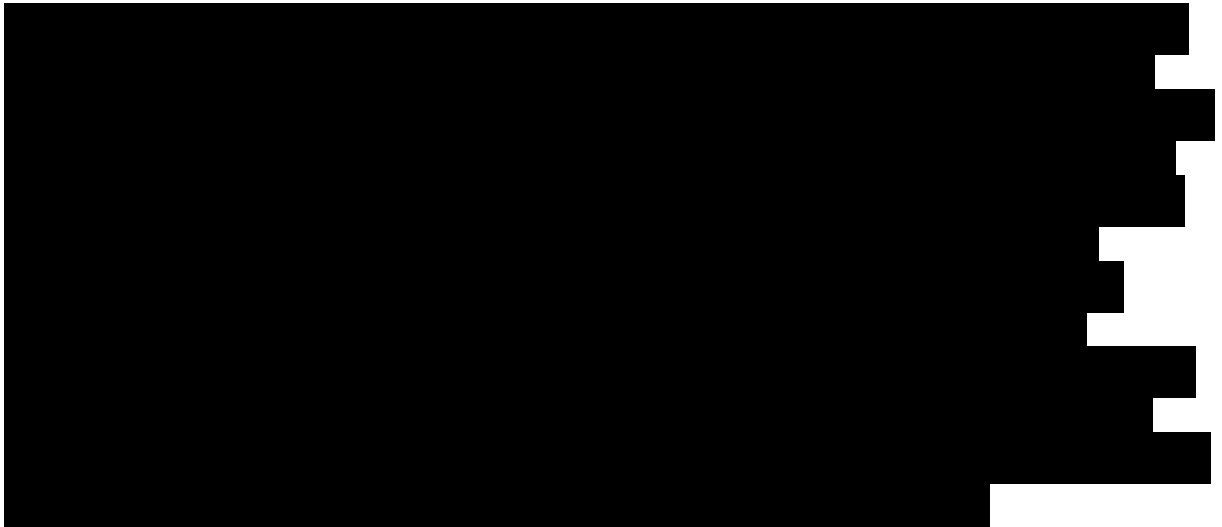
The sponsor has not studied the effect of extrinsic factors on PK of sestamibi.

2.5 General Biopharmaceutics

N/A

3.0 Detailed Labeling Recommendations:

The following labeling language is recommended under section “8- Use in specific patients: 8-4. Pediatric Use”:



[REDACTED]

[REDACTED]

[REDACTED]

[REDACTED]

[REDACTED]

[REDACTED]

[REDACTED]

[REDACTED]

[REDACTED]

[REDACTED]

[REDACTED]

[REDACTED]

[REDACTED]

[REDACTED]

[REDACTED]



[REDACTED]

[REDACTED]

[REDACTED]

[REDACTED]

[REDACTED]

[REDACTED]

[REDACTED]

[REDACTED]

[REDACTED]

[REDACTED]
 [REDACTED]
 [REDACTED]
 [REDACTED]
 [REDACTED]

[REDACTED]
 [REDACTED]

[REDACTED]

[REDACTED]
 [REDACTED]

[REDACTED]

[REDACTED]
 [REDACTED]

[REDACTED]

[REDACTED]

[REDACTED]	[REDACTED]	[REDACTED]	[REDACTED]	[REDACTED]	[REDACTED]
[REDACTED]	[REDACTED]	[REDACTED]	[REDACTED]	[REDACTED]	[REDACTED]
[REDACTED]	[REDACTED]	[REDACTED]	[REDACTED]	[REDACTED]	[REDACTED]
[REDACTED]	[REDACTED]	[REDACTED]	[REDACTED]	[REDACTED]	[REDACTED]
[REDACTED]	[REDACTED]	[REDACTED]	[REDACTED]	[REDACTED]	[REDACTED]
[REDACTED]	[REDACTED]	[REDACTED]	[REDACTED]	[REDACTED]	[REDACTED]

[REDACTED]

[REDACTED]

[REDACTED]

[REDACTED]

[REDACTED]

[REDACTED]

[REDACTED]

[REDACTED]

[REDACTED]

[REDACTED]

[REDACTED]

[REDACTED]

[REDACTED]

[REDACTED]

[REDACTED]

[REDACTED]

[REDACTED]

[REDACTED]

[REDACTED]

[REDACTED]

[REDACTED]

[REDACTED]

[REDACTED]

[Redacted]

- [Redacted]
- [Redacted]
- [Redacted]
- [Redacted]
- [Redacted]
- [Redacted]
- [Redacted]
- [Redacted]
- [Redacted]
- [Redacted]

[Redacted]

[REDACTED]

[REDACTED]

[REDACTED]

[REDACTED]

[REDACTED]

[REDACTED]

[REDACTED]

[REDACTED]

[REDACTED]

[REDACTED]

[REDACTED]

[REDACTED]

[REDACTED]

[REDACTED]

[REDACTED]

[REDACTED]

[REDACTED]

[REDACTED]

[REDACTED]

The most frequent exercise stress test endpoints sufficient to stop the test reported during controlled

[REDACTED]

[REDACTED]

[REDACTED]

[REDACTED]

[REDACTED]

[REDACTED]

[REDACTED]

[REDACTED]

[REDACTED]

[REDACTED]

[REDACTED]				
[REDACTED]				
[REDACTED]	[REDACTED]	[REDACTED]	[REDACTED]	[REDACTED]
[REDACTED]	[REDACTED]	[REDACTED]	[REDACTED]	[REDACTED]
[REDACTED]	[REDACTED]	[REDACTED]	[REDACTED]	[REDACTED]
[REDACTED]	[REDACTED]	[REDACTED]	[REDACTED]	[REDACTED]
[REDACTED]	[REDACTED]	[REDACTED]	[REDACTED]	[REDACTED]
[REDACTED]	[REDACTED]	[REDACTED]	[REDACTED]	[REDACTED]
[REDACTED]	[REDACTED]	[REDACTED]	[REDACTED]	[REDACTED]
[REDACTED]	[REDACTED]	[REDACTED]	[REDACTED]	[REDACTED]
[REDACTED]	[REDACTED]	[REDACTED]	[REDACTED]	[REDACTED]
[REDACTED]	[REDACTED]	[REDACTED]	[REDACTED]	[REDACTED]
[REDACTED]	[REDACTED]	[REDACTED]	[REDACTED]	[REDACTED]
[REDACTED]	[REDACTED]	[REDACTED]	[REDACTED]	[REDACTED]
[REDACTED]	[REDACTED]	[REDACTED]	[REDACTED]	[REDACTED]
[REDACTED]				

[REDACTED]

[REDACTED]

[REDACTED]

[REDACTED]

[REDACTED]

[REDACTED]

[REDACTED]

[REDACTED]

[Redacted]

[Redacted]

[Redacted]

[Redacted]

”

[REDACTED]

[REDACTED]

[REDACTED]

[REDACTED]

[REDACTED]

[REDACTED]

[REDACTED]

[REDACTED]

[REDACTED]

[REDACTED]

[REDACTED]

[REDACTED]

[REDACTED]

[REDACTED]

[REDACTED]

[REDACTED]

[REDACTED]

[REDACTED]

[REDACTED]

[REDACTED]

[REDACTED]

[REDACTED]

[REDACTED]

[REDACTED]

[REDACTED]

[REDACTED]

[REDACTED]

[REDACTED]

[REDACTED]

[REDACTED]

[REDACTED]

The table consists of approximately 15 rows of data. Each row is completely obscured by a solid black horizontal bar. The bars vary in length, suggesting different data points or categories. The redaction covers the entire content of the table, leaving no text or numbers visible.

Table 7.0

[Redacted text block]

[Redacted text block]

[Redacted text block]

[Redacted text block]

[Redacted text block]

[Redacted text block]

[Redacted text block]

[Redacted text block]

[REDACTED]

[REDACTED]

[REDACTED]

[REDACTED]

[REDACTED]			
[REDACTED]	[REDACTED]	[REDACTED]	[REDACTED]
[REDACTED]	[REDACTED]	[REDACTED]	[REDACTED]
[REDACTED]	[REDACTED]	[REDACTED]	[REDACTED]

[REDACTED]

[REDACTED]

[REDACTED]

[REDACTED]

[REDACTED]

[REDACTED]

[REDACTED]

[REDACTED]

[REDACTED]

[Redacted]

[Redacted]

[REDACTED]			
[REDACTED]	[REDACTED]	[REDACTED]	[REDACTED]
[REDACTED]	[REDACTED]	[REDACTED]	[REDACTED]
[REDACTED]	[REDACTED]	[REDACTED]	[REDACTED]
[REDACTED]	[REDACTED]	[REDACTED]	[REDACTED]

[REDACTED]			
[REDACTED]	[REDACTED]	[REDACTED]	[REDACTED]
[REDACTED]	[REDACTED]	[REDACTED]	[REDACTED]
[REDACTED]	[REDACTED]	[REDACTED]	[REDACTED]
[REDACTED]	[REDACTED]	[REDACTED]	[REDACTED]

[REDACTED]

[REDACTED]

[REDACTED]

[REDACTED]

[REDACTED]

[REDACTED]

[REDACTED]

[REDACTED] [REDACTED]

[REDACTED]

[REDACTED] [REDACTED] [REDACTED]

[REDACTED]

[REDACTED]

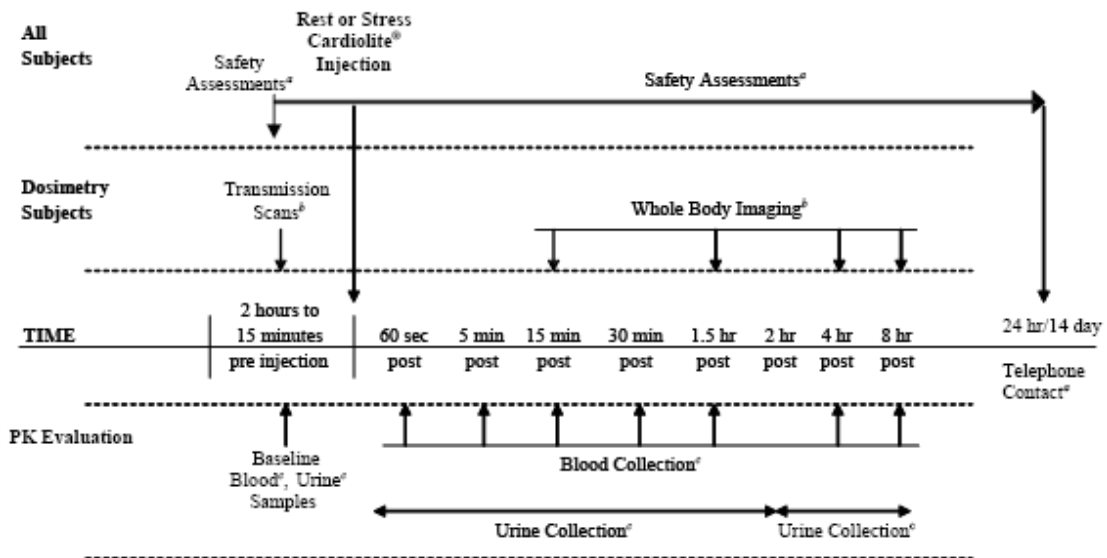
[REDACTED]

4.2 Individual Study Review:

The primary objective of this study was to determine the absorbed radiation dose of Cardiolite® (at rest or stress) in 2 pediatric subject age groups (children 4 to 11 years of age and adolescents 12 to 16 years of age). The secondary objectives of this study was to determine the biodistribution of Cardiolite® (at rest or stress) in children (age 4 to 11 years) and adolescents (age 12 to 16 years) and to determine the safety of Cardiolite® (at rest or stress) in children (age 4 to 11 years) and adolescents (age 12 to 16 years).

This was a Phase 1/2 open-label, non-randomized, multicenter trial in pediatric subjects who were scheduled to undergo a SPECT rest and/or stress Cardiolite® imaging study. Investigators were to enroll a minimum of 24 subjects into 2 age groups — children (age 4 to 11 years) and adolescents (age 12 to 16 years) — so that a minimum of 12 subjects were enrolled into each age group, and within each age group, a minimum of 6 subjects were to be studied after resting injection and 6 were to be studied after the stress injection. Ultimately, 79 subjects were enrolled due to methodology issues related to blood and urine sample collection and PK analysis with the initially enrolled subjects. All subjects were monitored for safety from the time of Cardiolite® injection until the 24 ± 12 hours telephone contact for adverse events (AEs) and for 14 days post-imaging for serious adverse events (SAEs).

The study plan is shown below in the cartoon:



This study was conducted in subjects already scheduled for a clinically indicated rest or stress SPECT Cardiolite® study, there was no additional radiation exposure solely for the purposes of this study beyond the very small exposure due to the transmission portion of the acquisition. All but 1 site enrolled subjects utilizing 1-day SPECT Cardiolite® imaging (either rest/stress or stress/rest). For these subjects, all study procedures were performed after the first injection of Cardiolite® (rest or stress) up through 8 ± 2 hours post-injection. Administration of the second dose of Cardiolite® to complete the clinically indicated cardiac imaging study occurred after all study-related procedures, including blood and urine collection, physical examination, and whole-body imaging (if applicable) were completed. The remaining site utilized a 2-day stress/rest protocol, performing all study-related procedures after the second dose of Cardiolite® (rest study).

For 47 Dosimetry Evaluable (DE) subjects, the largest mean estimated organ absorbed dose in this study was to the upper large intestine (ULI) wall at 0.082 mSv/MBq (0.30 rem/mCi). The next largest absorbed organ doses in decreasing order were to the small intestine (SI) wall at 0.043 mSv/MBq (0.16 rem/mCi), to the gall bladder wall at 0.042 mSv/MBq (0.16 rem/mCi), and to the lower large intestine wall at 0.035 mSv/MBq (0.13 rem/mCi). Significant differences were observed in liver, ULI contents, and SI contents between rest and stress subjects (liver: $p=0.026$; ULI: $p=0.015$; SI: $p=0.0002$) and between children and adolescents (liver: $p<0.0001$; ULI: $p=0.0016$; SI: $p<0.0001$). The average effective-dose equivalent (EDE) for Cardiolite®, which was a measure of stochastic risk, was estimated to be 0.019 mSv/MBq (0.072 rem/mCi). The average effective dose (ED) for Cardiolite®, which was also a measure of stochastic risk, was estimated to be 0.015 mSv/MBq (0.055 rem/mCi). Mean ED was significantly higher in children than in adolescents ($p<0.0001$). Similarly, mean EDE was significantly higher in children than in adolescents ($p<0.0001$).

Rest/stress effect was significant in the models of residence time in the liver ($p=0.0025$), SI contents ($p=0.0015$), and ULI ($p=0.002$). This was consistent with the visual observations of shifts of radioactivity between rest and stress studies in the organs of the hepatobiliary pathway.

For percent injected dose (%ID) corrected for radioactive decay, myocardial %ID reached a value of approximately 1.5% to 2% at 15 minutes after injection, decreasing to about 1.2% at 4 hours. In lungs, the %ID was low, with a maximum of approximately 4.6% at 15 minutes after injection. Similar %ID values in the myocardium and lung were obtained between all analysis groups. Liver %ID was similar in both children and adolescents, but significant differences ($p<0.0001$) were observed between rest and stress. In rest subjects, the %ID in the liver decreased rapidly from a maximum of approximately 26% at 15 minutes to less than 9% at 90 minutes. With stress, values decreased from 15% at 15 minutes to 7% at 90 minutes.

Significant differences between rest and stress of a similar magnitude were also observed ($p=0.0002$) in the SI contents.

For the 46 Pharmacokinetic Evaluable (PE) subjects in this study, the radioactivity following Cardiolite® administration had similar blood PK profiles in children and adolescents, whereas the profiles were significantly different between rest and stress subjects ($p=0.0013$). The mean %ID in whole body blood volume (WBBV) was 53.5% at 1 minute in stress subjects followed by a rapid decline to 5.1% at 5 minutes, compared to that of 28.4% at 1 minute and 5.4% at 5 minutes in rest subjects. A similar trend was observed in 18 subjects in the DE + PE population. The mean \pm standard deviation (SD) of the blood PK parameters for the PE population, area under the blood concentration-time curve from zero to the time of last quantifiable concentration [AUC (0-T)], area under the blood concentration-time curve from time zero extrapolated to infinite time [AUC (INF)], terminal elimination blood half life (T1/2), and mean residence time (MRT), are summarized in the table 1 for the 4 analysis groups:

Table I. PK parameters for Cardiolite in pediatric subjects

Analysis Groups	AUC(0-T) (%ID hr) Mean (SD)	AUC(INF) (%ID hr) Mean (SD)	Terminal T1/2 (hr) Mean (SD)	MRT (hr) Mean (SD)
Rest Children (n = 13)	5.21 (1.81)	6.86 (2.85)	3.50 (1.20)	3.73 (1.35)
Rest Adolescents (n = 14)	4.04 (1.37)	5.13 (1.65)	3.13 (0.84)	3.51 (1.12)
Stress Children (n = 10)	6.11 (1.97)	8.20 (3.07)	4.13 (1.19)	4.22 (1.32)
Stress Adolescents (n = 9)	5.43 (1.32)	6.66 (1.82)	3.10 (1.17)	2.96 (1.19)
Overall (n = 46)	5.09 (1.76)	6.59 (2.59)	3.45 (1.13)	3.62 (1.27)

The overall PK parameters for radioactivity in blood following Cardiolite administration were an AUC(0-T) of 5.09 ± 1.76 %ID.hr, AUC(INF) of 6.59 ± 2.59 %ID.hr, terminal elimination T1/2 of 3.45 ± 1.13 hours, and MRT of 3.62 ± 1.27 hours. Higher AUC values were observed in stress subjects [AUC(0-T): $p=0.019$; AUC(INF): $p=0.04$] and in children [AUC(0-T): $p=0.0497$; AUC(INF): $p=0.026$] with differences that were statistically significant. No

significant differences were observed in terminal elimination T1/2 and MRT values.

The overall mean urinary excretion of radioactivity by 6 hours was $13.8 \pm 8.59\%$, with the majority recovered during the first 2 hours post-Cardiolite® administration.

Dosimetry: Radiation dosimetry was calculated by the core laboratory, [REDACTED] and the results were grouped by rest or stress study type and age category (adolescent or child), yielding 4 analysis groups.

The study presented an overview of methods, as well as results in terms of relative radioactivity for selected organs at each time point, summary data for residence times, and summary statistics for organ-by-organ radiation dose, ED, and effective-dose equivalent (EDE). Details of the dosimetry calculations, including region definitions, results for individual subjects, and results in both traditional and standard international units, as well as quality control and other operational and methodological details of the analysis are contained in the Core Laboratory Report.

Radiation dosimetry estimates for individual organs were calculated from analysis of whole-body image data taken at four time points after injection. Anterior and posterior whole-body Cardiolite® conjugate images were obtained with a dual-head gamma camera using Cardiolite® at nominal times of 15 minutes, 1.5 hours, 4 hours, and 8 hours. In addition, transmission and reference scans were obtained prior to dose administration using an external cobalt-57 (^{57}Co) “flood” source to allow calculation of gamma ray absorption factors. A small reference source was included in each whole-body scan as a check on scanning parameter. Image data were then transferred to the core laboratory for all subsequent analysis.

Image data were quantified based on the Medical Internal Radiation Dose (MIRD) methodology and consistent with MIRD Pamphlet 16 (Siegel et al., 1999). Regions of interest (ROI) were drawn around the whole body and around all organs that showed uptake above background, including gall bladder contents, small intestine (SI) contents, ULI contents, lower large intestine (LLI) contents, heart wall, kidneys, liver, lungs, salivary glands, spleen, thyroid, and urinary bladder contents. For purposes of region-drawing, the whole body was segmented into sub-regions of approximately equal anterior-posterior thickness. The geometric mean of corresponding region sums from the anterior and posterior emission whole-body images was calculated. Attenuation correction factors were derived from regions applied to the transmission image and the transmission reference image.

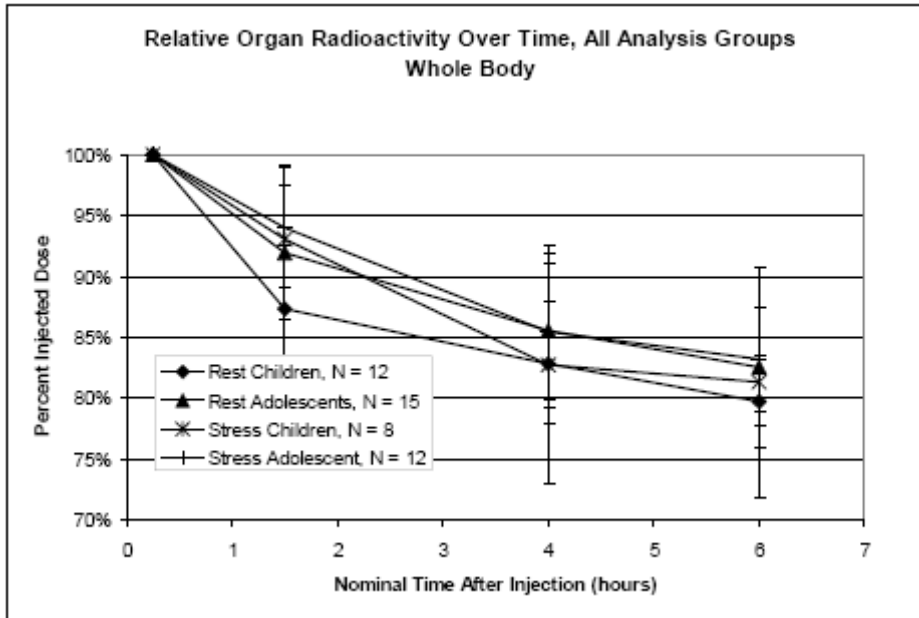
Region counts were adjusted for activity contained in underlying and overlying tissue that was not part of the organ or tissue being quantified. This was done using adjacent “background” regions with appropriate corrections for relative thickness. Total body region counts were also corrected for off body background counts. Appropriate normalization of region sizes for organ and adjacent regions were made. For organs that contained excess activity due to overlap of other organs or tissues, regions were drawn over unobstructed areas and the count density multiplied by the total area of the organ with the excess activity. Region data from the transmission image and reference transmission image were used to create correction factors for gamma ray attenuation in tissue. Organ thickness values required for determining attenuation correction factors were taken from the Cristy-Eckerman pediatric phantoms (Cristy and Eckerman, 1987), and interpolated based on the individual subject’s height and mass.

Absorbed dose estimates for Cardiolite® were then produced from the Cristy-Eckerman phantoms, and the standard MIRD methodology, using Organ Level Internal Dose Assessment/EXponential Modeling (OLINDA/EXM). The MIRD methodology, developed over many years, begins with the tabulated, published results of radiation absorption and transport calculations within and between organs created using mathematical abstractions of human anatomy (called phantoms) at a variety of ages. These are combined with the characteristics of the isotope used and kinetic data derived from imaging studies to calculate estimates of radiation dose. The resulting values are referred to as estimates because they pertain only to the generalized human beings represented by the phantoms, rather than to any individual, but are considered sufficiently accurate for diagnostic radiopharmaceuticals.

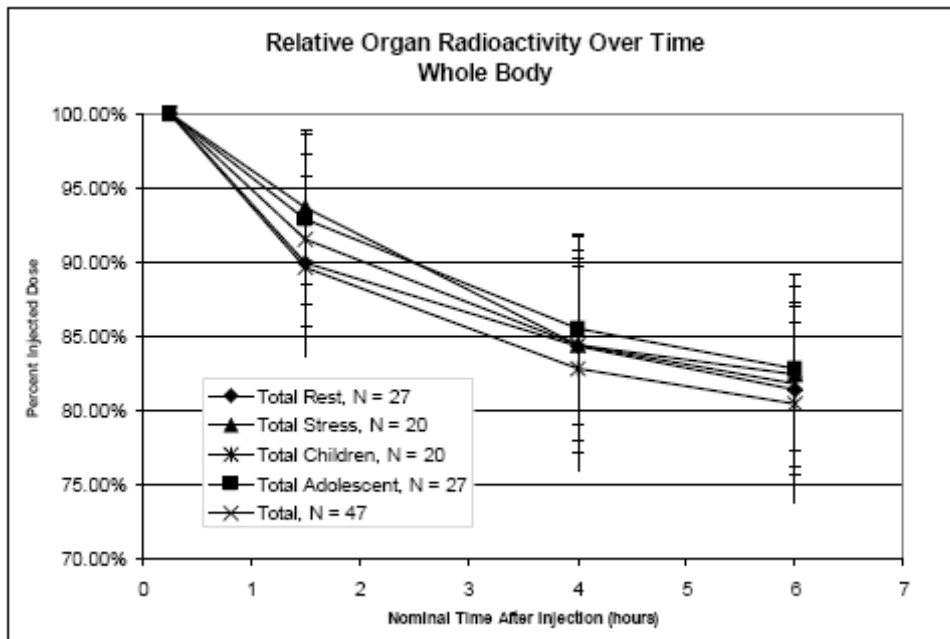
Mean residence Time:

It can be seen that there was relatively little difference between the values for children and those of adolescents. However, significant differences were observed in residence times of liver ($p=0.0025$), SI contents ($p=0.0015$), and ULI contents ($p=0.002$) between rest and stress subjects, reflecting the shift of compound localization under stress conditions. Although not statistically significant, similar, smaller differences were seen in the gall bladder and LLI. The remainder of the body, which represented all other radioactivity not specifically accounted for in the other organs, increased, reflecting the shift away from the bowel in the stress studies that was not compensated for by increases in other specifically visualized organs. This may indicate generally increased localization in skeletal muscle and other structures under stress conditions.

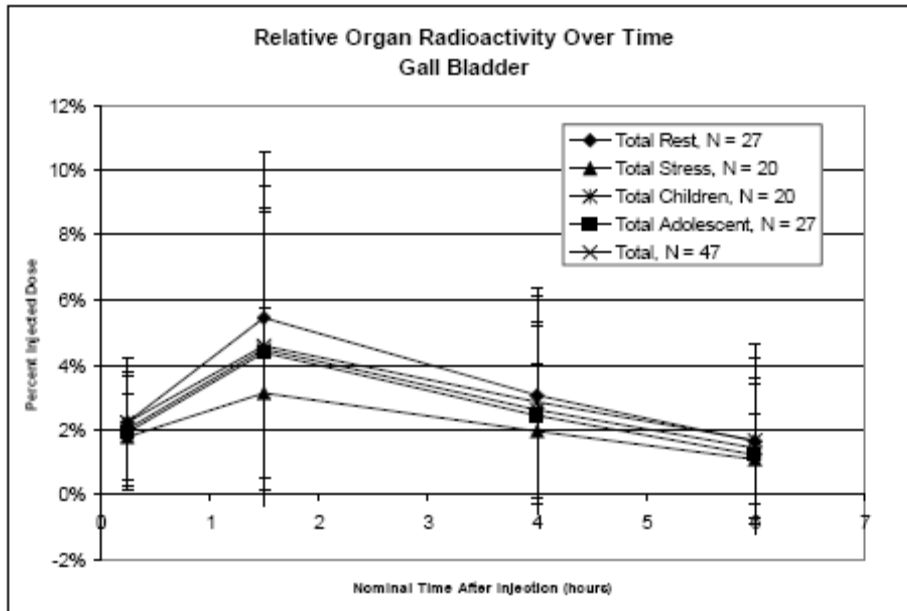
Time-activity curves for various organs at rest and stress are shown below for children and adolescents.



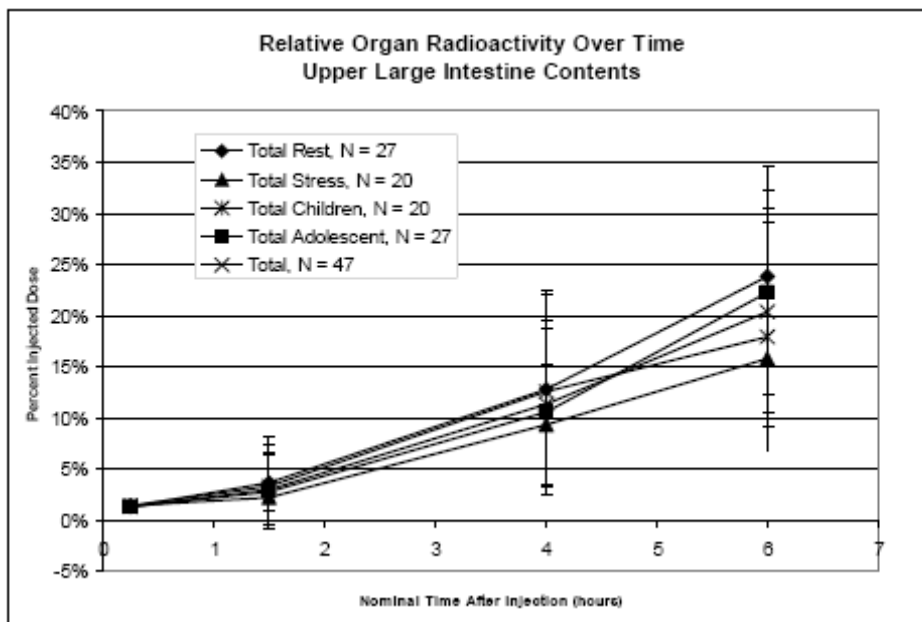
Mean Decay-Corrected %ID in the whole body, resting and stress studies, adolescent and children and all subjects.



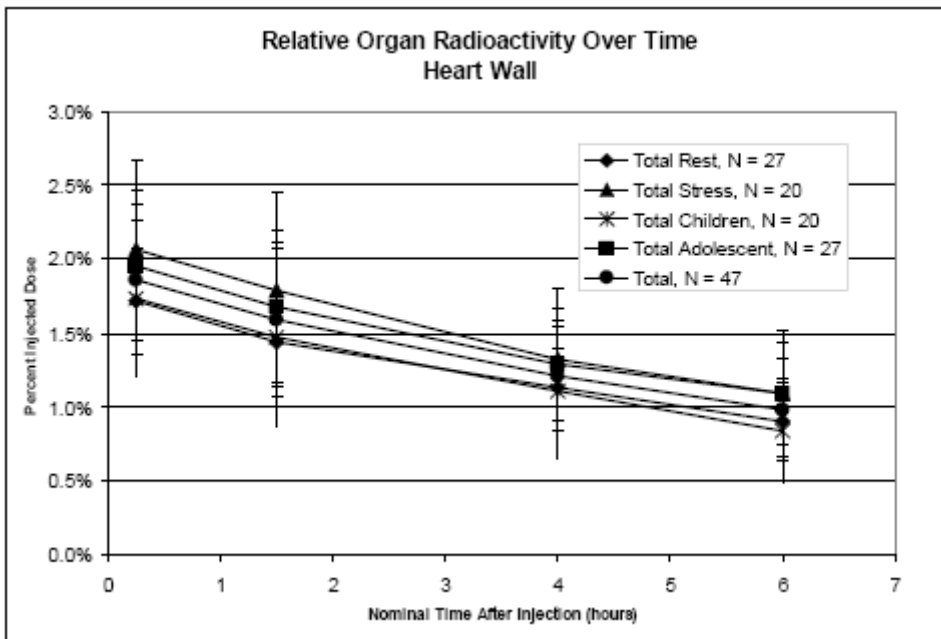
Mean Decay-Corrected %ID in gall bladder, resting and stress studies, adolescent and children and all subjects.



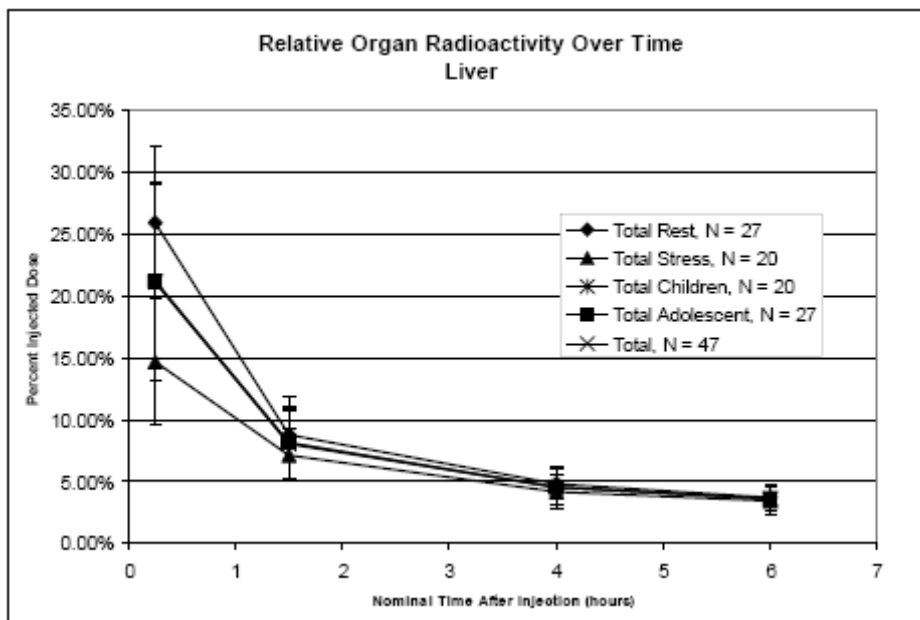
Mean Decay-Corrected %ID in upper large intestine, resting and stress studies, adolescent and children and all subjects.



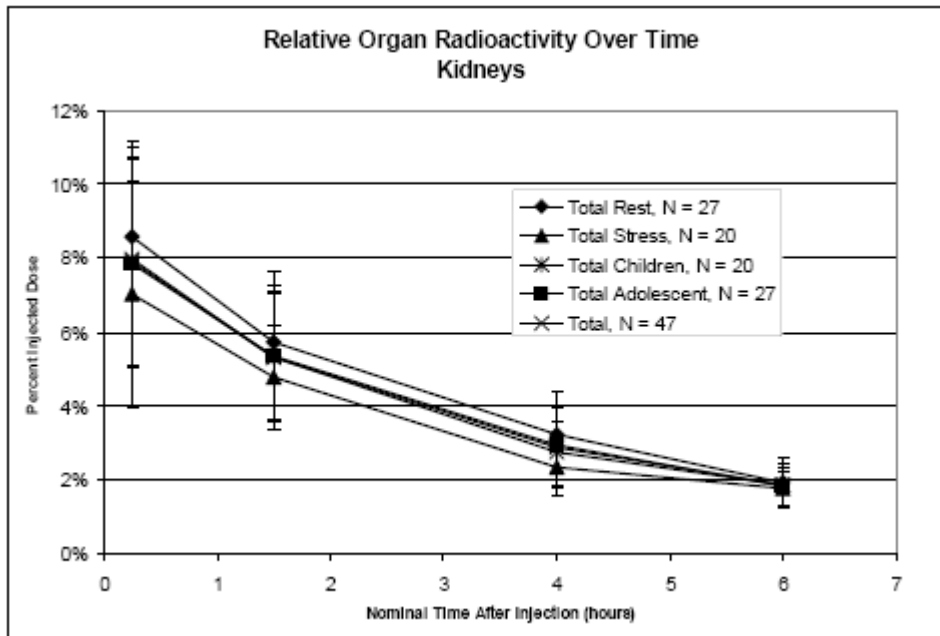
Mean Decay-Corrected %ID in heart wall, resting and stress studies, adolescent and children and all subjects.



Mean Decay-Corrected %ID in liver, resting and stress studies, adolescent and children and all subjects.



Mean Decay-Corrected %ID in kidney, resting and stress studies, adolescent and children and all subjects.



These data demonstrate that the excretion of Cardiolite® was divided between the renal and hepatobiliary pathways, with the remainder deposited throughout the body. The organs with relatively larger residence times tended to be the larger organs in the body, as this quantity represented the total number of disintegrations in a given organ, and therefore reflected both the concentration of the radioactivity and the mass of the organ. The organs with larger mass were the remainder of the body, red marrow, liver, and lungs. The other structures with larger residence times were primarily the excretory organs, the bowel, and urinary bladder contents.

Absorbed Dose estimates:

Overall, the organs receiving the highest doses were those that formed the hepatobiliary excretion pathway: the ULI wall, with 0.082 mSv/MBq, the SI wall with 0.043 mSv/MBq, the gall bladder wall with 0.042 mSv/MBq, and the LLI wall with 0.035 mSv/MBq. The next highest dose was seen in the wall of the urinary bladder at 0.027 mSv/MBq.

4.3. Consult Reviews

N/A

**This is a representation of an electronic record that was signed electronically and
this page is the manifestation of the electronic signature.**

/s/

Christy John
4/30/2008 12:06:18 PM
BIOPHARMACEUTICS

Young-Moon Choi
4/30/2008 12:08:43 PM
BIOPHARMACEUTICS

Atiqur Rahman
4/30/2008 01:21:10 PM
BIOPHARMACEUTICS